Mechanical unfolding of single filamin A (ABP-280) molecules detected by atomic force microscopy

Shou Furuike[a], Tadanao Ito[b], Masahito Yamazaki[a,c,*]

[a] *Materials Science, Graduate School of Science and Engineering, Shizuoka University, 836 Oya, Shizuoka 422-8529, Japan*
[b] *Department of Biophysics, Graduate School of Science, Kyoto University, Kyoto 606-8502, Japan*
[c] *Department of Physics, Faculty of Science, Shizuoka University, 836 Oya, Shizuoka 422-8529, Japan*

Received 26 February 2001; revised 2 May 2001; accepted 8 May 2001

First published online 17 May 2001

Edited by Amy M. McGough

Abstract Filamin A (ABP-280), which is an actin-binding protein of 560 kDa as a dimer, can, together with actin filaments, produce an isotropic cross-linked three-dimensional network (actin/filamin A gel) that plays an important role in mechanical responses of cells in processes such as maintenance of membrane stability and translational locomotion. In this study, we investigated the mechanical properties of single filamin A molecules using atomic force microscopy. In force–extension curves, we observed sawtooth patterns corresponding to the unfolding of individual immunoglobulin (Ig)-fold domains of filamin A. At a pulling speed of 0.37 μm/s, the unfolding interval was sharply distributed around 30 nm, while the unfolding force ranged from 50 to 220 pN. This wide distribution of the unfolding force can be explained by variation in values of activation energy and the width of activation barrier of 24 Ig-fold domains of the filamin A at the unfolding transition. This unfolding can endow filamin A with great extensibility. The refolding of the unfolded chain of filamin A occurred when the force applied to the protein was reduced to near zero, indicating that its unfolding is reversible. Based on these results, we discuss here the physiological implications of the mechanical properties of single filamin A molecules.

Key words: Cytoskeleton; Actin/filamin A gel; Mechanical unfolding; Mechanical response of cell; Atomic force microscopy

1. Introduction

The actin cytoskeleton is thought to play important roles in the formation of various kinds of structures of cell membranes, the mechanical response of cells, and cell locomotion. Actin filaments and a large number of F-actin cross-linking proteins can form various kinds of structures, such as bundles and isotropic three-dimensional (3-D) networks. Filamin A (ABP-280) is one of these F-actin cross-linking proteins. It is present at the leading edge and cortex of many kinds of non-muscle cells such as fibroblasts, cerebral cortical neurons, platelets, and macrophages [1–5]. This protein can produce isotropic cross-linked 3-D networks with actin filaments (F-actin) in vivo and in vitro [1,2,6,7]. In this report, we describe such networks as actin/filamin A (actin/ABP-280) gel. Filamin A can also link the actin cytoskeleton to plasma membrane via its association with integral membrane proteins such as β1 and β2 integrin [8,9], a tissue factor, presenilin, furin, Ibα in platelets, and a receptor for the F_c domain of immunoglobulin (Ig) G (FcγR1).

Filamin A-deficient melanoma cells have impaired locomotion and exhibit circumferential blebbing of plasma membrane [10,11]. Mutations in filamin A prevent long-range, directed migration of cerebral cortical neurons to the cortex in human periventricular heterotopica [4]. Filamin A and actin filaments accumulate at membrane cortices that are under high membrane tension to increase the strength of the cortex for mechanoprotection [12]. These results suggest that filamin A and actin/filamin A gel play an important role in the mechanical properties of cells and cell locomotion.

Human endothelial filamin A is a dimeric protein with equivalent 280-kDa subunits that associate with each other at their C-terminal domain. It has two N-terminal actin-binding sites per dimer, and can thus cross-link actin filaments. Most of this protein (90%) is a semiflexible rod composed of 24 tandem repeats, each containing 96 amino acids on average, and its amino acid sequence predicts stretches of antiparallel β-sheets in an Ig-fold [3]. A similar Ig-fold was found in a filamin (gelation factor, or ABP-120) in *Dictyostelium discoideum*, and the 3-D structure of segment 4 of its rod domain was determined using nuclear magnetic resonance spectroscopy [13].

In this study, we investigated the mechanical properties of single filamin A molecules using atomic force microscopy (AFM). Recent studies have shown that AFM can detect the unfolding of proteins during extension by measuring external force in aqueous solutions [14–18]. Applying the methods used in these studies, we have found that single molecules of human endothelial filamin A are unfolded by critical external forces of various intensities, and that its unfolding is reversible; i.e. the refolding of the unfolded chain of filamin A occurs when the external force is removed. Based on these results, we discuss the physiological implications of the mechanical properties of single filamin A molecules.

2. Materials and methods

Filamin A was purified from human uterine leiomyoma tissue by gel filtration with a 4% agarose column [7]. Ruby mica (diameter, 14 mm; thickness, 300 ± 20 μm) was purchased from S&J Trading Inc. (Glen Oaks, NY, USA). Gold wires (99.99% pure; 1φ × 10 mm) were purchased from Furuya metal (Tokyo, Japan).

We used a Nanoscope IIIa Multimode AFM (MMAFM) (Digital

*Corresponding author. Fax: (81)-54-238 4741.
E-mail: spmyama@ipc.shizuoka.ac.jp

0014-5793/01/$20.00
PII: S0014-5793(01)02497-8

Instruments, Santa Barbara, CA, USA) equipped with a D scanner (12 μm × 12 μm × 4.4 μm) and a fluid cell. For the cantilever, we used an oxide-sharpened Si_3N_4 cantilever (NP-S) with a spring constant of $k = 0.06$ N/m (Digital Instruments). The gold-coated mica substrate used in the AFM experiment was prepared by deposition of gold on a freshly cleaved mica surface using a vacuum deposition apparatus (VPC-410, Sinku Kiko Co., Yokohama, Japan), and the thickness of the gold layer was 100 nm. Filamin A protein molecules in aqueous solution in 10 mM imidazole–HCl (pH 7.5), 0.1 M KCl, and 0.5 mM EGTA (protein concentration, 70 μg/ml) were adsorbed onto a freshly evaporated gold surface on the mica substrate for 10 min. When a lower protein concentration was used, the probability of adsorbing the protein molecule on the AFM tip was lower, but the pattern of the force–extension curve was independent of the protein concentration. After the surface was washed with the same imidazole buffer to remove the unadsorbed proteins, the AFM tip was brought to the gold surface and the force–extension curve was measured.

The Monte Carlo simulation of the unfolding of Ig-fold domains was performed according to the method of Rief et al. [19]. In the simulation, a protein (i.e. polypeptide chain) is stretched with a constant pulling speed v_c from extension $x = 0$ by a small amount Δx ($= v_c \Delta t$) at each time interval. This stretching increases the force exerted on the protein, which is calculated based on the worm-like chain (WLC) model (Eq. 1). The probability of observing the unfolding of any Ig-fold domains at this force is then calculated as described in Section 3, and then random number decision is executed to define their states. We used values of parameters: $v_c = 0.4$ μm/s, $p = 0.4$ nm, the length of the Ig-fold domain in the folded state ($I_f = 4$ nm) and that in the unfolded state ($I_u = 36$ nm). This Monte Carlo simulation produces a force–extension curve ($0 \leq x \leq 500$ nm), showing the sawtooth pattern.

3. Results and discussion

In order to investigate the mechanical properties of a single molecule of filamin A protein, we stretched the molecule in aqueous solution and measured its force–extension relationship at room temperature using an AFM apparatus. After adsorbing the protein molecules on the gold surface, the AFM tip was brought to the gold surface and kept there for 2 s with a force of 100 pN ~ 1 nN to adsorb the segments of the filamin A protein, after which the tip was pulled away. In the retraction curves, we often observed a large attractive force between the tip and the gold surface to a large extension, sometimes more than 500 nm. This indicates that the filamin A molecule adsorbed on both the tip and the gold surface was stretched as the distance between the tip and the gold surface increased (i.e. extension). In most cases, we observed a periodic increase and decrease in force during the extension; i.e. so-called sawtooth pattern of the force–extension curve (Fig. 1a). With small extensions, before the appearance of the sawtooth pattern in the extension curve, an irregular large attractive force which was not well-defined was often observed (e.g. curve (ii) of Fig. 3). At a pulling speed of 0.4 μm/s, the maximum force and the periodicity of the sawtooth patterns were 100 ~ 200 pN and 30 ± 5 nm, respectively. As well-analyzed in reports of the stretching of titin and its analogue proteins [14,17], the abrupt decrease in force in the sawtooth patterns corresponds to the force-induced unfolding of an individual Ig-fold domain of filamin A.

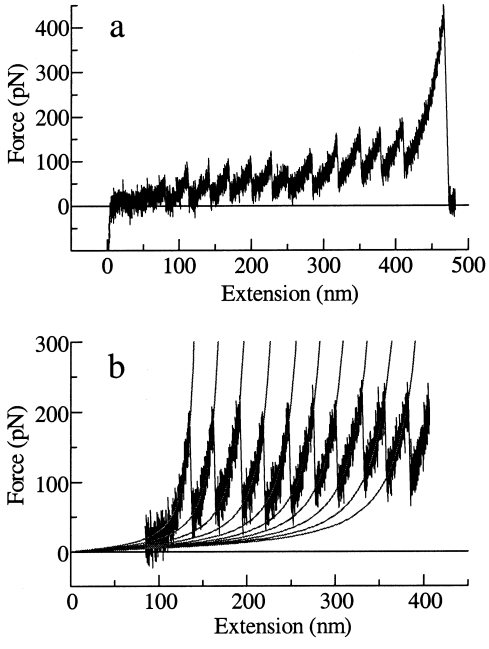

Fig. 1. (a) A force–extension curve of filamin A molecule in aqueous solution measured by AFM at room temperature. Filamin A was stretched at a pulling speed of 0.37 μm/s. (b) The fit between the WLC model and the sawtooth pattern of the force–extension curve where the force gradually increased after the abrupt decrease in force. Filamin A was stretched at a pulling speed of 0.37 μm/s.

In the sawtooth patterns, immediately after the abrupt decrease in force due to the unfolding of the Ig-fold domain, the force again gradually increased with increasing extension. As shown in Fig. 1b, the force, $F(x)$, vs. extension, x, curve of this part of the sawtooth pattern is described well by the WLC model, as follows:

$$F(x) = \frac{k_B T}{p}\left\{\frac{1}{4}\left(1-\frac{x}{L_c}\right)^{-2}-\frac{1}{4}+\frac{x}{L_c}\right\} \quad (1)$$

where p is persistence length and L_c is contour length. The best fit gave $p = 0.33$ nm and ΔL_c (i.e. the change in contour length between consecutive force peaks) $= 31 \pm 1$ nm. This result shows that the force–extension curve of the unfolded polypeptide chain can be described well by the WLC model, indicating that the force that increases with increasing extension is an entropic force due to the stretching of the unfolded polypeptide chain of filamin A. When the force reaches the critical intensity by extending the unfolded chain, an unfolding transition of another Ig-fold domain of filamin A is induced. This characteristic change in force was repeated several times in the force–extension curve, resulting in the sawtooth pattern.

The force at which the unfolding occurs is defined as the unfolding force, F^*. As shown in Fig. 1a, F^* had various values. Fig. 2a shows a histogram of the unfolding force of filamin A at a pulling speed of 0.37 μm/s when it was pulled up until $x = 500$ nm ($n = 214$ unfolding events). The unfolding force F^* ranged from 50 to 220 pN. On the other hand, a histogram of the unfolding interval (i.e. the periodicity of the sawtooth patterns) of filamin A in Fig. 2b exhibited a narrow distribution around an average value of 30 nm. This indicates that the successive unfolding of Ig-fold domains in either of two identical subunits of filamin A should give such a wide distribution pattern of the unfolding force as shown in Fig. 2a.

To investigate the cause of the wide distribution in the unfolding force of filamin A, we performed a Monte Carlo simulation of the unfolding of this protein. The mechanical unfolding of proteins can be explained as a non-equilibrium

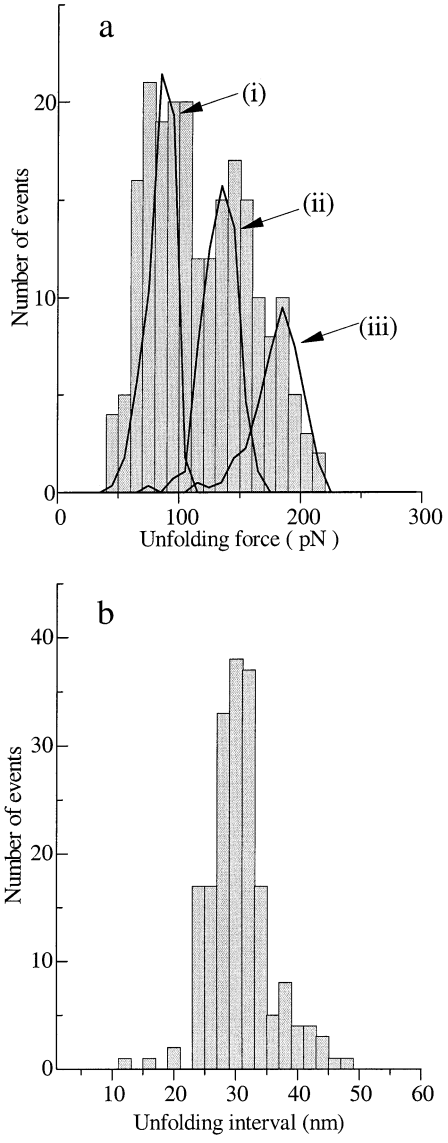

Fig. 2. (a) A histogram of the unfolding force of the Ig-fold domains of filamin A at the pulling speed of 0.37 μm/s ($n=214$ unfolding events from 24 independent experiments). The three curves correspond to the unfolding force obtained from Monte Carlo simulations of 20 Ig-fold domains with different structures, as characterized by two parameters (k_u^0 and x_u). Curve (i), $x_u=0.5$ nm and $k_u^0=3.0\times10^{-4}$ s^{-1}; curve (ii), $x_u=0.4$ nm and $k_u^0=3.0\times10^{-5}$ s^{-1}; curve (iii), $x_u=0.3$ nm and $k_u^0=3.0\times10^{-5}$ s^{-1}. (b) A histogram of the unfolding interval of filamin A, obtained from the same data sets used to construct the unfolding force histogram (a).

process of transition between two states, i.e. a native state and an unfolded state. The rate of transition from the native state to the unfolded state (i.e. the unfolding rate) in the absence of the force, k_u^0, depends on activation energy (energy barrier), E_u^0, and is given by the following equation:

$$k_u^0 = A\exp(-E_u^0/k_BT) \quad (2)$$

where k_B is Boltzmann's constant and T is temperature. External force, F, reduces the energy barrier by Fx_u, where x_u is the width of the activation barrier (i.e. the distance to the transition state along the direction of force) [19,20], and the unfolding rate $k_u(F)$ is thus expressed as follows:

$$k_u(F) = A\exp(-(E_u^0-Fx_u)/k_BT) = k_u^0\exp(Fx_u/k_BT) \quad (3)$$

The transition between the two states is a stochastic process that can be simulated well by the Monte Carlo method [17,20]. The probability of observing the unfolding of any modules is $P_u=N_fk_u(F)\Delta t$, where N_f is the number of identical folded modules and Δt is the polling interval of the Monte Carlo simulation. During unfolding by force, folding of the unfolded chain does not occur [17]. In this model, the probability of mechanical unfolding of protein can be determined using only two parameters related to the protein structure; i.e. the activation energy E_u^0 and the width of the activation barrier, x_u. The k_u^0 and x_u values were determined for proteins consisting of a finite number of identical domains, such as $I27_8$ (the eight tandem repeats of the 27th Ig-fold domain of human cardiac titin prepared using a recombinant DNA technique); $x_u=0.25$ nm and $k_u^0=3.3\times10^{-4}$ s^{-1}. The stochastic nature of the unfolding transition contributes to the width of the histograms of the unfolding force of the proteins [17,21]. However, the width of the histogram of the unfolding force of filamin A (Fig. 2a) is much broader than that of $I27_8$, and the distribution function of the unfolding force in the histogram of filamin A cannot be represented as the kind of simple distribution function observed for $I27_8$. This indicates that there is broad heterogeneity in the unfolding forces of filamin A.

Recently, Li showed that point mutations in a different amino acid of $I27_8$ affected the mechanical stability significantly: k_u^0 ranged from 8.0×10^{-7} to 3.3×10^{-4} s^{-1} due to the variation in values of the activation energy E_u^0 in each mutant protein, and the width of the activation barrier, x_u, ranged from 0.25 to 0.60 nm [21]. Thus, we can reasonably assume that each Ig-fold domain of filamin A has different values of E_u^0 (and, therefore, k_u^0) and x_u, because the individual Ig domains of filamin A have different amino acid sequences. To demonstrate the effects of k_u^0 and x_u on the unfolding force of the Ig-fold domain, in Fig. 2a we plotted three curves obtained from Monte Carlo simulations of 20 identical Ig-fold domains having different structures, as characterized by two parameters (k_u^0 and x_u): curve (i), $x_u=0.5$ nm and $k_u^0=3.0\times10^{-4}$ s^{-1}; curve (ii), $x_u=0.4$ nm and $k_u^0=3.0\times10^{-5}$ s^{-1}; curve (iii), $x_u=0.3$ nm and $k_u^0=3.0\times10^{-5}$ s^{-1}. These curves fit well into parts of the histogram in Fig. 2a. Such heterogeneity in the unfolding force of filamin A can yield a wide dynamic range in the force needed to extend the molecule, suggesting that, in the mechanical responses of cells, the extension of filamin A may be suitably adjusted by forces of various intensities.

Fig. 3 shows a refolding of the unfolded Ig-fold domains of filamin A. After several Ig-fold domains of filamin A were unfolded during the large extension caused by the external force, the AFM tip was brought to a position 44 nm above the gold surface, to relax the protein to almost its initial length and reduce the force to near zero. After holding the tip at that position for 10 s, the protein was stretched again (the second stretch). As shown in the figure, most of the sawtooth patterns reappeared in the second stretch, indicating that most of the unfolded domains were refolded by this procedure, i.e. the unfolding was reversible. In another similar

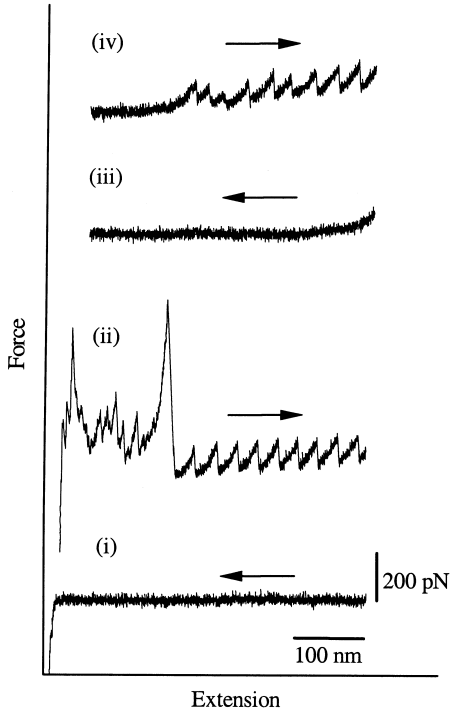

Fig. 3. Refolding of the unfolded filamin A protein. The AFM tip was brought to the gold surface and kept there for 2 s to adsorb the protein onto its tip (curve (i)). The filamin A was then stretched (curve (ii)), and the characteristic sawtooth pattern appeared. After the extension, the AFM tip was brought to a position 44 nm above the gold surface to reduce the force to near zero (curve (iii)). After holding there for 10 s, the protein was stretched again (curve (iv)). The pulling speed and the approach speed were both 0.40 μm/s.

experiment, after the filamin A was unfolded during the initial large extension, the AFM tip was brought to a position 40 nm above the gold surface and held at that position for 1 s instead of 10 s, after which the protein was stretched again. This time, fewer sawtooth patterns reappeared during the large extension in the second stretch (data not shown), suggesting that it takes time for the unfolded domains to refold.

The F-actin network cross-linked by filamin A (actin/filamin A gel) shows the following characteristic properties in vitro (Ito et al., manuscript in preparation). At low shear strains ($\gamma < 20\%$), it behaves as a linearly deforming gel; at moderate shear strains ($20\% < \gamma < 100\%$), it behaves as a non-linearly deforming gel with deformability that increases with increasing shear strain; at high shear strains ($\gamma > 100\%$), it behaves as a non-Newtonian fluid. In addition, its rheological properties show reversibility; after the removal of a large shear strain, the rheological properties return to their original values.

Cross-linking of actin filaments by filamin A may suppress the undulation motion of the actin filaments in the network [22]. A relatively large shear force imposed on the network would induce a stepwise unfolding of filamin A as reported here, and this unfolding of the cross-linker should bring about a gradual increase in the undulation motion of the filaments. Such a change of the undulation motion of the filaments and the reversibility of the unfolding of the cross-linker may well account for the characteristic rheological properties of the network described above. This actin/filamin A network, which constructs cortical shell of non-muscle cells, may play an essential role in the mechanical responses of cells to external deformation. The above-described in vitro responses of the actin/filamin A network suggest that cells can stabilize their shapes against a small shear force, and that their deformability increases against a large shear force.

Acknowledgements: This work was supported in part by a Grant-in-Aid for General Scientific Research C from the Ministry of Education, Science, and Culture, Japan.

References

[1] Hartwig, J.H. and Stossel, T.P. (1981) J. Mol. Biol. 145, 563–581.
[2] Hartwig, J.H. and Shevlin, P. (1986) J. Cell Biol. 103, 1007–1020.
[3] Gorlin, J.B., Yamin, R., Egan, S., Stewart, M., Stossel, T.P., Kwiatkowski, D.J. and Hartwig, J.H. (1990) J. Cell. Biol. 111, 1089–1105.
[4] Fox, J.W., Lamperti, E.D., Ekçioglu, Y.Z., Hong, S.E., Feng, Y., Graham, D.A., Scheffer, I.E., Dobyns, W.B., Hirsch, B.A., Radtke, R.A., Berkovic, S.F., Huttenlocher, P.R. and Walsh, C.A. (1998) Neuron 21, 1315–1325.
[5] Stossel, T.P., Condeelis, J., Cooley, L., Hartwig, J.H., Schleichen, M. and Shapiro, S.S. (2001) Nat. Rev. Mol. Cell Biol. 2, 138–146.
[6] Janmey, P.A., Hvidt, S., Lamb, J. and Stossel, T.P. (1990) Nature 345, 89–92.
[7] Ito, T., Suzuki, A. and Stossel, T. (1992) Biophys. J. 61, 1301–1305.
[8] Sharma, C.P., Ezzell, R.M. and Arnaout, M.A. (1995) J. Immunol. 154, 3461–3470.
[9] Loo, D.T., Kanner, S.B. and Aruffo, A. (1998) J. Biol. Chem. 273, 23304–23312.
[10] Cunningham, C.C., Gorlin, J.B., Kwiatkowski, D.J., Hartwig, J.H., Janmey, P.A., Byers, H.R. and Stossel, T.P. (1992) Science 255, 325–327.
[11] Cunningham, C.C. (1995) J. Cell Biol. 129, 1589–1599.
[12] Glogauer, M., Arora, P., Chou, D., Janmey, P.A., Downey, G.P. and McCulloch, C.A.G. (1998) J. Biol. Chem. 273, 1689–1698.
[13] Fucini, P., Renner, C., Herberhold, C., Noegel, A.A. and Holak, T.A. (1997) Nat. Struct. Biol. 4, 223–231.
[14] Rief, M., Gautel, M., Oesterhelt, F., Fernandez, J.M. and Gaub, H.E. (1997) Science 276, 1109–1112.
[15] Ikai, A., Mitsui, K., Furutani, Y., Hara, M., McMurty, J. and Wong, K.P. (1997) Jpn. J. Appl. Phys. 36, 3887–3893.
[16] Oberhauser, A.F., Marszalek, P.E., Erickson, H.P. and Fernandez, J.M. (1998) Nature 393, 181–185.
[17] Carrion-Vazquez, M., Oberhauser, A.F., Fowler, S.B., Marszalek, P.E., Broedel, S.E., Clarke, J. and Fernandez, J.M. (1999) Proc. Natl. Acad. Sci. USA 96, 3694–3699.
[18] Carl, P., Kwok, C.H., Manderson, G., Speicher, D.W. and Discher, D.E. (2001) Proc. Natl. Acad. Sci. USA 98, 1565–1570.
[19] Rief, M., Fernandez, J.M. and Gaub, H.E. (1998) Phys. Rev. Lett. 81, 4764–4767.
[20] Evans, E. and Ritchie, K. (1997) Biophys. J. 72, 1541–1555.
[21] Li, H., Carrion-Vazquez, M., Oberhauser, A.F., Marszalek, P.E. and Fernandez, J.M. (2000) Nat. Struct. Biol. 7, 1117–1120.
[22] Morse, D.C. (1998) Macromolecules 31, 7044–7067.